

First principles study of the spin state transitions in $\text{GdBaCo}_2\text{O}_{5.5}$

V. Pardo^{1,2,*} and D. Baldomir^{1,2}

¹ *Departamento de Física Aplicada, Facultad de Física, Universidad de Santiago de Compostela, E-15782 Campus Sur s/n, Santiago de Compostela, Spain*

² *Instituto de Investigaciones Tecnológicas, Universidad de Santiago de Compostela, E-15782, Santiago de Compostela, Spain*

Electronic structure calculations were carried out on the compound $\text{GdBaCo}_2\text{O}_{5.5}$. The electronic structure variation with a change in the spin state of the Co^{3+} ion in an octahedral environment has been studied. All the insulating phases are described and possible scenarios for the metallic ones are presented. Orbital ordering is shown to take place and the electronic structure leading to it is determined. The Ising-like anisotropy shown experimentally can be predicted. Also, big unquenched orbital angular momenta are calculated and their origin is described.

PACS numbers: 71.20.-b, 71.30.+h, 75.50.Pp

I. INTRODUCTION

Co oxides have been the objective of deep research during the last few years. As any correlated oxide, they present an interplay between the electronic structure, magnetic properties and geometric structure that makes them very interesting from both an experimental and a theoretical point of view. They have received a strong attention very recently, mainly after the discovery of both superconductivity¹ and magnetoresistance² in them because of the vast technological applications of those phenomena, but also because of the magnetic transitions accompanied of structural transitions, that are not yet fully understood. $\text{GdBaCo}_2\text{O}_{5.5}$ presents magnetic transitions at about 75 and 220 K and a metal-insulator transition at some 360 K.³ The magnetization measurements at the different phases have not been conclusively ascribed to a particular spin state and orbital configuration. There are no measurements available of the orbital magnetic moments of the Co ions in the different phases and spin states. This rich variety of phases including spin state transitions occurs in Co^{3+} compounds, where the low-spin state is not stable at all temperatures because of the small magnitude of the crystal field, comparable to the intra-atomic exchange energy. This is the case of $\text{GdBaCo}_2\text{O}_{5.5}$, that also presents giant magnetoresistance² associated with a metal-insulator transition. Very recently, a spin blockade phenomenon has been found to explain its conduction properties.^{4,5} Some work has also been carried out from a theoretical standpoint.^{6,7,8,9} The goal of this paper is to make use of electronic structure calculations in order to explain the magnetic and electronic structure of the compound and their variations with respect to the magnetic and spin state transitions that occur in it. For doing so, in section II we will describe the structure of the material and the method of calculation and in section III we will present our calculations of the magnetic and electronic structure, dealing with the spin state, magnetic and metal-insulator transitions, and also with the orbital ordering phenomenon relating all of these to the macroscopic observations establishing a consistent picture for

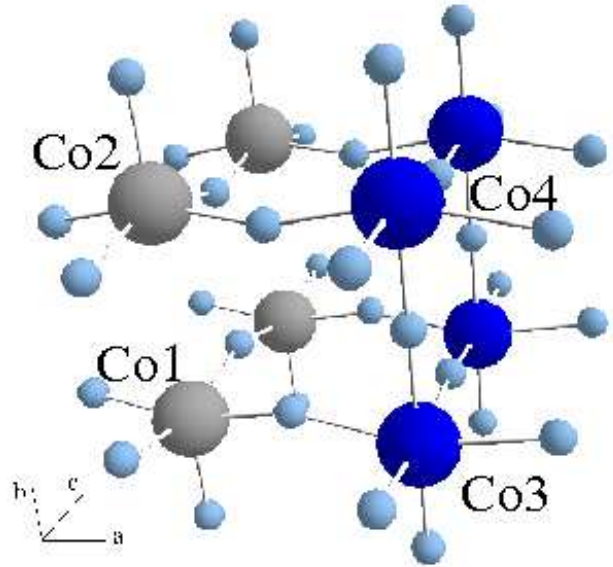


FIG. 1: (Color online) Structure of $\text{GdBaCo}_2\text{O}_{5.5}$. Grey atoms (Co1 and Co2) are Co_{pyr} , dark atoms (Co3 and Co4) are Co_{oct} and the small light ones are the oxygen atoms. Observe the oxygen vacants along the c -axis leading to a square pyramidal environment.

the observed properties of the material.

II. STRUCTURE AND COMPUTATIONAL DETAILS

$\text{GdBaCo}_2\text{O}_{5.5}$ presents two crystallographically different surroundings for the two inequivalent Co ions in the unit cell. One of them is in a square pyramidal (Co_{pyr}) and the other in an octahedral environment (Co_{oct}). There is one oxygen vacant per unit cell, that produces the square pyramidal environment for the Co in the crystallographic position 2r. The octahedron surrounding Co_{oct} is elongated along the a -axis (see Fig. 1 for the naming of the crystallographic directions). The unit cell

is orthorhombic with space group Pmmm. The value of the lattice parameters and atomic positions were taken from Respaud *et al.*¹⁰ ($a= 3.87738$ Å, $b= 7.53487$ Å and $c= 7.8269$ Å), but the oxygen positions were recalculated performing a full structural relaxation. It is well established that the oxygen vacants are in the crystallographic position 1g (1/2, 1/2, 1/2).¹⁰ For our calculations we broke the symmetry along the b-axis, so that 4 inequivalent Co atoms enter the cell (let us call Co1 and Co2 the two inequivalent atoms in the pyramidal position and Co3 and Co4 the two inequivalent atoms in the octahedral environment, as can be seen in Fig. 1). Further symmetry breakings were produced along the c- and a-axis to have 8 Co atoms in the supercell: the former case with the intention of studying possible spin state orderings in the yz plane and the latter for analyzing the magnetic couplings between Co_{pyr} layers mediated by a plane of Co_{oct} atoms.

TABLE I: Crystallographic positions at T= 0 that result from our structure optimization.

Atom	Crystallographic position	Coordinates
Ba	2σ	(0,0,0.2503)
Gd	2p	(0,0.5,0.2292)
Co_{pyr}	2r	(0.5,0.2563,0.5)
Co_{oct}	2q	(0.5,0.2487,0)
O1	1a	(0.5,0,0)
O2	1e	(0.5,0,0.5)
O3	1c	(0.5,0.5,0)
O4	2s	(0,0.2731,0)
O5	2t	(0,0.3102,0.5)
O6	4u	(0.5,0.2947,0.2633)

We present here full-potential, all-electron, electronic structure calculations based on the density functional theory (DFT) utilizing the APW+lo method¹¹ performed with the WIEN2k software.^{12,13} For the structure minimization, the results of which are summarized in Table I, we used the GGA (generalized gradient approximation) in the Perdew-Burke-Ernzerhoff (PBE) scheme.¹⁴ The geometry optimization was carried out minimizing the forces in the atoms and the total energy of the system. These results are independent of the magnetic ordering, forces are minimized both in the case of ferromagnetic (FM) or antiferromagnetic (AF) ordering. Also, a force minimization procedure was carried out in a supercell containing 8 inequivalent Co atoms. Minimal changes of the atomic positions compared to those reported in Table I turn out as a result. For the electronic structure calculations, we included the strong correlation effects by means of the LDA+U scheme¹⁵ in the so-called “fully-localized limit”.¹⁶ The values of U chosen were within the range of 3 to 6 eV for all the spin states (U depends on the spin state of the atom) but all the results presented here are fully consistent for U within that range (the quantitative results of energy differences depend on the choice of U by

some 25% for values of U within that range, the values presented will be given for U= 4.5 eV). Spin-orbit effects have been introduced in a second variational way using the scalar relativistic approximation.¹⁷ The parameters of our calculations depend on the type of calculation but for any of them we converged with respect to the k-mesh and to $R_{mt}K_{max}$, up to 1000 k-points (256 in the irreducible Brillouin zone) and up to $R_{mt}K_{max}= 7$. Local orbitals were added for a bigger flexibility in dealing with the semicore states. Muffin-tin radii chosen were the following: 2.3 a.u. for both Ba and Gd, 1.90 a.u. for Co and 1.59 a.u. for O.

III. ELECTRONIC AND MAGNETIC STRUCTURE

From a purely ionic point of view, we expect both Co^{3+} ions in a d^6 configuration, that in an octahedral environment could lead to either a low spin (LS) state ($t_{2g}^6 e_g^0$; nonmagnetic S=0), an intermediate spin (IS) state ($t_{2g}^5 e_g^1$; S=1) or even a high spin (HS) state ($t_{2g}^4 e_g^2$; S=2). Spin state transitions play an important role in the temperature evolution of the electronic, structural and magnetic properties of transition metal oxides, specially in the case of Co^{3+} compounds, such as the famous example of LaCoO_3 .¹⁸ In the case of $\text{GdBaCo}_2\text{O}_{5.5}$, it is not yet clearly understood the relationship between a spin state transition and the transition from AF to FM behavior¹⁹ (neither with the metal-insulator transition).²⁰ We have studied in this paper how the electronic structure evolves with spin states and our calculations always relax to a scenario with Co_{pyr} in the IS state, not being possible the stabilization of a different spin state for that atom. Usually, the pyramidal sites of $\text{GdBaCo}_2\text{O}_{5.5}$ have been ascribed to the IS state,^{21,22} even crystal field arguments confirm it as being very stable.³ Very recently, a spin blockade phenomenon was found to explain the conduction properties of the material,⁴ being its origin explainable assuming an IS state in Co_{pyr} atoms.⁵ However, some works evidence that a HS state is likely to occur for a Co^{3+} ion in a square pyramidal environment in some cases, as has been evidenced by neutron diffraction,^{23,24} spectroscopy measurements,²⁵ and also theoretically^{8,26,27} for different materials containing similar environments for a Co^{3+} ion. Even for $\text{GdBaCo}_2\text{O}_{5.5}$, calculations^{6,7} and theoretical results⁹ show a HS state as the most stable for Co_{pyr} , contrary to our results. However, all the solutions we tried converge to an IS state of Co_{pyr} indicating an enormous stability of such a state. The different results obtained with similar methods could be due to our structure optimization, that leads to changes of up to 2% in interatomic distances and bond angles with respect to the experimental room temperature data. It is well-known that variations in the geometry of the cation environment could lead to the stabilization of a different spin state.²⁸ Also, the LDA+U method is strongly dependent on the starting point and several

solutions can be obtained depending on the starting density chosen. On the other hand, for Co_{oct} , different spin states could be converged: a LS state, an IS state and a spin state order with half the Co_{oct} atoms in a HS state and the other half in a LS state. A HS state of Co_{oct} could not be converged with the structural data we utilized. It has been shown experimentally that a structural transition¹⁰ occurs at the metal-insulator transition and this has been related to the appearance of a HS state. Such a HS state would stabilize through a strong spin-lattice coupling that our zero temperature DFT calculations cannot describe.

A. Magnetic ordering and magnetic transitions

We have studied several magnetic and spin configurations within the LDA+U approximation. Both FM and AF couplings along the three crystallographic directions have been considered. Our calculations yield a FM coupling along the *b*- and *c*-axis as the most stable one for any spin state of the Co_{oct} layer. Within each of the layers, an AF ordering cannot be stabilized. It has been argued³ that orbital ordering produces the stabilization of a FM ordering within the plane, and that is what we observe (see Section III B). For the case of a LS state of the Co_{oct} atoms, a FM and an AF ordering of Co_{pyr} layers mediated by a nonmagnetic Co_{oct} layer were calculated. AF ordering is more stable by some 10 meV/Co (*U*-dependent value but consistent for a wide set of *U* choices), not a strong magnetic coupling. Both IS-LS solutions (IS stands for the spin state of Co_{pyr} and LS for the spin state of the Co_{oct} atoms), consisting of planes coupled AF or FM, lead to an insulating behavior (see Fig. 2). We observe that the IS-LS configuration leads to a zero-gap insulator, in accordance with experiments observing a narrow gap.²⁹ This is the only solution that could explain the properties of the AFI (antiferromagnetic insulator) phase found below 70 K. The weak magnetic coupling between the layers breaks up at that temperature entering the paramagnetic phase above it.

From our calculations, we interpret the AF-FM transition that occurs at about 220 K as a change in the magnetic coupling of FM Co_{pyr} layers mediated by nonmagnetic Co_{oct} planes, because such a FM ordering is the only one leading to a FMI (ferromagnetic insulator) phase. This is consistent with the experimental observations in Ref. 3.

The magnetic coupling between Co_{oct} and Co_{pyr} layers when the former acquires an IS state is FM. The energy difference between a FM and an AF configuration is about 40 meV/Co (*U*-dependent value), a strong magnetic coupling. We could also converge a FM solution where half of the Co_{oct} atoms are in a HS state and the other half in a LS state, a spin state ordering situation, similar to what has been observed for $\text{NdBaCo}_2\text{O}_{5.5}$ ³⁰ (in this case it has been predicted to be between IS and LS states) or predicted theoretically for the whole

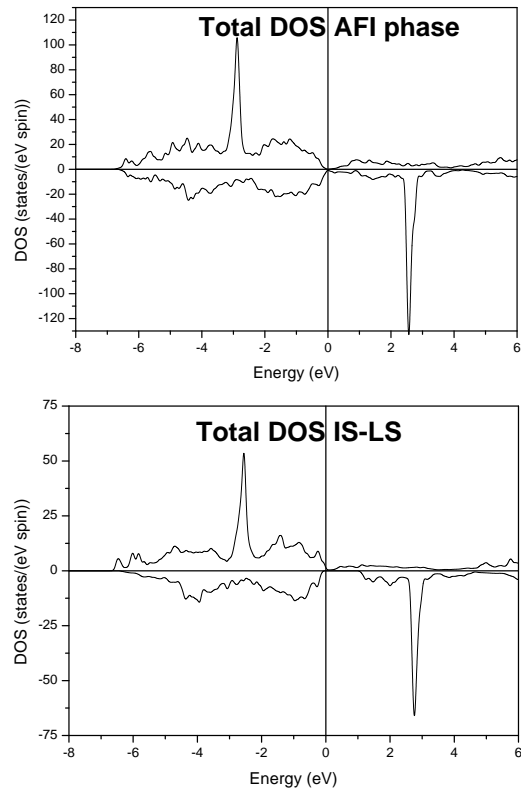


FIG. 2: Spin-up and spin-down total DOS plots for the material in the insulating phases, when the Co_{oct} atoms are in a LS state. The upper panel shows an AF coupling between Co_{pyr} layers and the lower panel shows a FM situation.

series⁹ (but in that case the authors assume that Co_{pyr} possesses a HS). These two solutions we have computed lead to a half-metallic state (see Fig. 3). In principle, any of these could be the magnetic ordering in the metallic phase above the metal-insulator transition. But, since a structural deformation has been observed experimentally at the metal-insulator transition¹⁰ and this has been ascribed to the onset of a HS state, we should not rule out the possibility of a HS Co_{oct} layer above the metal-insulator transition. The structural data we utilized (calculated at $T=0$) does not allow to stabilize that configuration. The calculation of such a phase by DFT techniques would require a precise knowledge of the geometry above 360 K. The recent magnetization measurements³ observing a total magnetic moment of $1 \mu_B/\text{Co}$ above the metal-insulator transition would rule out this possibility. As we will see below, orbital angular momenta need to be taken into account for explaining the total magnetization measurements.

B. Orbital ordering

Co^{3+} ions in an IS state have an orbital degree of freedom, that could lead to the existence of orbital order-

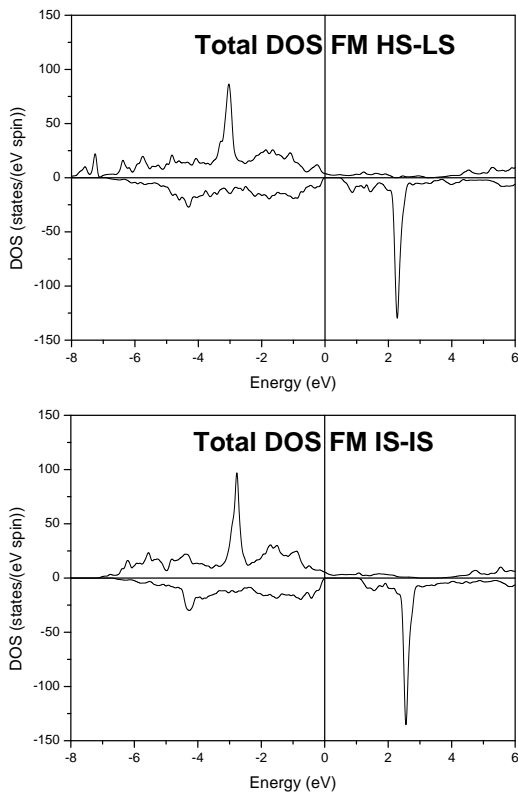


FIG. 3: Spin-up and spin-down total DOS plots for the material in the possible metallic phases considered in the text. The upper panel shows a spin state ordering HS-LS in the Co_{oct} layers and the lower panel shows an IS state for all the Co_{oct} atoms.

ing along the b and c -axes.^{29,31} The octahedral environment is elongated along the crystallographic c -axis (we will consider it here as our z -axis for the representation of the d -levels). For the pyramidal environment, the z -axis will be considered along the direction of the oxygen vacant (crystallographic b -axis). For Co_{pyr} , due to the small crystal field splitting a Co^{3+} ion suffers, an orbital degeneracy is likely to occur as well (depending on the intra-atomic exchange energy).

Let us first begin with the IS-LS situation, the ground state. Figs. 4 and 5 show the density of states (DOS) of the d -levels for the IS state of the Co_{pyr} atoms. Their electronic structure does not vary much when the spin state of Co_{oct} changes. According to our calculations, the IS state of Co_{pyr} is fairly stable and remains unchanged when increasing temperature, so our description of this state is valid for any spin state of the Co_{oct} atoms. We can observe in the curves a different electronic structure in the crystallographically equivalent Co atoms, indicating the existence of orbital ordering along the b -axis (the crystallographic axis that joins the two inequivalent Co_{pyr} (and also Co_{oct}) atoms we have considered in our calculations (see Fig. 1). In Ref. 31, this orbital state is predicted to be $d_{xz} \pm i d_{yz}$ for $\text{DyBaCo}_2\text{O}_{5.5}$, but we

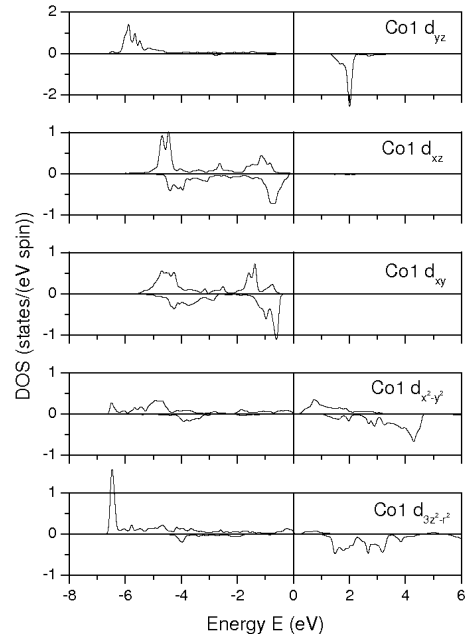


FIG. 4: Spin-up and spin-down partial density of states of $\text{Co}1$ (in a square pyramidal environment). It can be observed that it is in an IS state and the hole in the t_{2g} multiplet is in the d_{yz} orbital.

obtain as the ground state an orbital ordering between real orbitals (d_{xz} and d_{yz}), being this configuration some 20 meV/Co more stable than the state with equal orbital structure along the b -axis (even though the magnitude of the energy difference is dependent on the value of U chosen, the important point is that it certainly is more stable independently of U), a value comparable to the energy involved in magnetic ordering. Similar calculations indicate that the same orbital ordering is stable as well along the c -axis. Couplings within the bc -plane are equivalent both orbitally and magnetically. However, the location of the electron that is promoted into the e_g doublet is more difficult to ascribe, since it is not in a pure $d_{3z^2-r^2}$ nor in the $d_{x^2-y^2}$ orbital, as can be observed in Figs. 4 and 5. We also decomposed the DOS curves in a set of orbitals using the complex functions $d_{3z^2-r^2} \pm i d_{x^2-y^2}$ (consistent with having the same environment for both Co atoms, since these orbitals have cubic symmetry) but the electron does not fit into those orbitals alternately neither. Some more complicated orbital structure occurs that we could not discern with our calculations. We can only ascertain that the resultant states must have some component of each orbital, probably a complex combination since an unquenched orbital angular momentum occurs as we will see below. Also, the e_g bands (this is valid for Co_{oct} in an IS state as well) contain more than one electron, that probably comes from a very strong

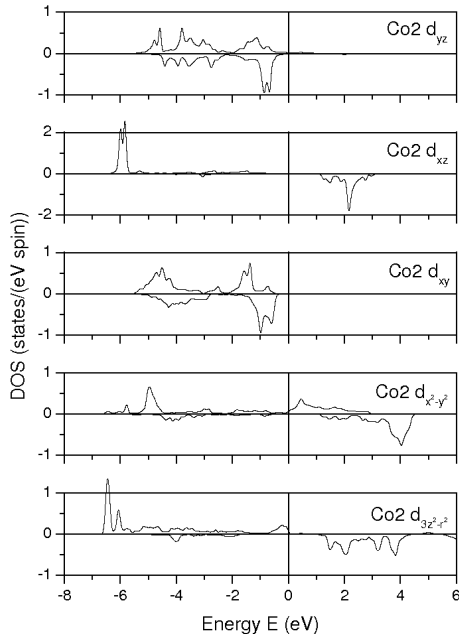


FIG. 5: Spin-up and spin-down partial density of states of Co2 (in a square pyramidal environment). It can be observed that it is in an IS state and the hole in the t_{2g} multiplet is in the d_{xz} orbital.

hybridization of the e_g band with the surrounding O p bands. This could imply the formation of a $\text{Co}^{2+}\underline{\text{L}}$ state ($\underline{\text{L}}$ being a ligand hole). This strong hybridization had been already found in previous works,^{6,32} but for a HS state of Co_{pyr} .

For the case of Co_{oct} , we present in Figs. 6 and 7 the d -DOS for the IS state. The plots of the LS state are not introduced because the electronic structure is basically a $t_{2g}^6 e_g^0$ configuration in a nearly octahedral environment, the t_{2g} levels fully occupied and the e_g levels fully unoccupied. In the IS state, one of the electrons in the lower lying multiplet is promoted to the e_g levels. There occurs an orbital ordering phenomenon as well for Co_{oct} in the IS state along the b -axis. The DOS of two contiguous Co_{oct} atoms along that direction are shown in Figs. 6 and 7, where it can be seen that the hole left in the t_{2g} multiplet is alternatively at the d_{xy} and d_{xz} orbitals. This configuration is some 10 meV/Co more stable than the non-orbitally ordered scenario (that energy value might vary slightly with the value of U chosen, but it is consistent for a wide range of U). The electron that is promoted in the e_g multiplet places in alternate orbitals, but from our calculations it is difficult to describe the combination of $d_{3z^2-r^2}$ and $d_{x^2-y^2}$ orbitals that forms the doublet. We know it is not the pure real orbitals as we can see in Figs. 6 and 7 but they are not the complex orbitals $d_{3z^2-r^2} \pm i d_{x^2-y^2}$ neither. We tried that possi-

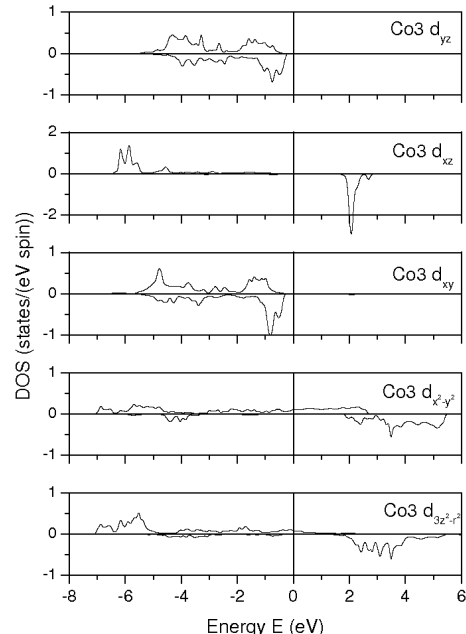


FIG. 6: Spin-up and spin-down partial density of states of Co3 (in an octahedral environment) for the IS-IS configuration. It can be observed that it is in an IS state and the hole in the t_{2g} multiplet is in the d_{xz} orbital.

bility decomposing our DOS in a basis containing those two orbitals but such an ordering was not found. Some other admixture of these orbitals is happening due to the local environment of the atom but from our calculations this could not be sorted out. We encounter here a similar situation to the case of Co_{pyr} , the fact that there exist some unquenched orbital angular momenta rules out the possibility of having real orbitals, the electron must be located in a state formed by some complex combination of orbitals. The e_g band is also in this case strongly hybridized, possibly forming a $\text{Co}^{2+}\underline{\text{L}}$ state as for Co_{pyr} . In an IS-IS situation, the orbital ordering was found to be stable both along the b - and c -axis, consistent with the picture established in Ref. 3.

In a spin state ordering situation, the Co_{oct} atom in a LS state acquires some magnetic moment due to the surrounding HS ions and the e_g bands become occupied forming a very wide band that crosses the Fermi level leading to the half-metallic behavior observed in Fig. 3.

C. Spin-orbit study: unquenched orbital angular momenta and magnetic anisotropy

We have also carried out calculations including spin-orbit coupling to elucidate how the magnetic anisotropy changes for the different spin states and magnetic cou-

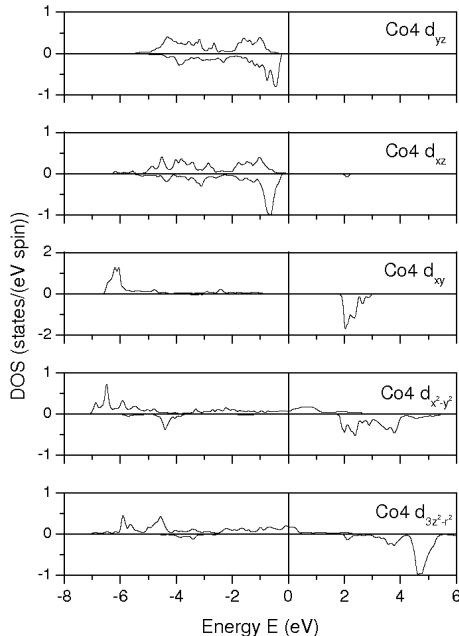


FIG. 7: Spin-up and spin-down partial density of states of Co4 (in an octahedral environment) for the IS-IS configuration. It can be observed that it is in an IS state and the hole in the t_{2g} multiplet is in the d_{xy} orbital.

plings and to evaluate the orbital angular momenta (OAM) of the different Co atoms in the structure, that had been predicted to have some unquenched OAM³¹ but whose values have never been measured. Only values of total magnetization are available in the literature,^{19,21,33} showing some discrepancies between them.

TABLE II: Values of the orbital angular momenta of the four Co atoms in the structure in the three spin state configurations studied. The values are given in μ_B and are considered inside the muffin-tin sphere. These values are calculated for the magnetization along the experimental easy axis.

Atom	IS-IS (μ_B)	IS-LS (μ_B)	IS-(HS-LS)(μ_B)
Co1 (pyr)	0.30	0.28	0.27
Co2 (pyr)	0.02	0.01	0.01
Co3 (oct)	0.01	-0.05	0.03 (LS)
Co4 (oct)	0.24	-0.07	0.19 (HS)

A summary of the OAM calculated is presented in Table II. These data are calculated assuming the magnetization goes along the experimental easy axis (c -axis). The values are given inside the muffin-tin spheres, so the real values of the moments are, hence, somewhat bigger (about 10-30%, but this is difficult to estimate). They also are U-dependent by up to 25% for other combinations of U parameters within a reasonable range. Large

values up to $0.6 \mu_B$ for some of the Co atoms would be consistent with our calculations. Experimental measurements are needed to confirm this observation. We performed these calculations for the three different spin state configurations we could converge for the Co_{oct} atoms (Co_{pyr} is always in an IS state): a LS, an IS state and a spin state ordering with half the Co_{oct} atoms in a HS state and the other half in a LS state.

Irrespective of the Co_{oct} spin state, we observe that Co_{pyr} atoms have very similar angular momenta (one of them being about $0.3 \mu_B$ inside the muffin-tin sphere). The electronic structure of these atoms barely changes when a spin state transition occurs to Co_{oct} . This atom develops a big angular momentum in one of the sites when it is in an IS state. It is worth noting that the big orbital angular momentum occurs when the hole in the t_{2g} multiplet is left in the d_{xz} orbital, both in the case of Co_{pyr} and Co_{oct} in an IS state, whereas the configuration with a hole in a different t_{2g} orbital produces a negligible moment. Small values are predicted also for Co_{oct} in a LS state. These are oppositely oriented to the magnetic moment of the Co_{pyr} ions when all the Co_{oct} atoms are in a LS state and parallel to them when the layer includes Co_{oct} atoms in a HS state. These also have a large value of the OAM, but smaller than those of the IS state.

We also performed calculations of the magnetic anisotropy energies and our results agree with the experimental data available.²⁹ We obtain a strong Ising-like behavior for the AFI phase (IS-LS with IS Co_{pyr} planes coupled AF via nonmagnetic Co_{oct} layers). In that case, the c -axis is the easy axis by some 150 K/Co, a big anisotropy energy, in agreement with the experimental value (some 80-100 K/Co).²⁹ For the IS-LS FMI phase, we find an easy axis along the c -axis, being the b -direction almost degenerate (3 K/Co harder) and the a -direction harder by some 40 K/Co. No trace of Ising-like behavior is found for this phase. This disagrees with the experimental findings because our zero-temperature DFT calculations cannot describe appropriately the magnetic anisotropy properties at 260 K, where they have been measured.²⁹ A similar situation occurs for the IS-IS FM state, the b -axis is the easy axis being the a and c directions harder by some 30 K/Co. In these cases it could be possible that the domain formation found in Ref. 3 could have an influence on the value of the magnetic anisotropy constants that is not considered in the calculation of the magnetocrystalline anisotropy energy.

IV. CONCLUSIONS

In this paper we have presented a study of the electronic structure and magnetic properties of the Co oxide $GdBaCo_2O_{5.5}$ using *ab initio* calculations considering an all-electron, full-potential APW+lo method. The points we tried to address were the spin state transitions, the orbital ordering and spin-orbit effects (unquenched orbital angular momenta and magnetic anisotropy proper-

ties). From our calculations we confirm the stability of the IS state for Co_{pyr} or the conduction properties of the IS-LS state as a narrow gap insulator. The transition to a metallic phase must be accompanied of a spin state transition of Co_{oct} . It is necessary to know the precise geometry in the metallic phase to determine its spin and magnetic configuration. We have observed the material is in an orbitally-ordered state both at low temperatures in the IS-LS state and also in a hypothetical IS-IS state, and we described the orbitals involved in the phenomenon. We also predict big unquenched orbital angular momenta for some of the Co atoms in the structure, a fact that had been predicted but whose values have never been measured. We estimate their values and explain their origin. Also, the magnetic anisotropy was

studied and agrees with the experimental observation of a strong Ising-like behavior. In summary, we establish a consistent picture for the properties of the material by confirming some experimental evidences and predicting new results based on first principles calculations.

Acknowledgments

The authors wish to thank the CESGA (Centro de Supercomputacion de Galicia) for the computing facilities and the Xunta de Galicia for the financial support through a grant and the project PGIDIT02TMT20601PR.

-
- * Electronic address: vpardo@usc.es
- ¹ K. Takada, H. Sakurai, E. Takayama-Muromachi, F. Izumi, R. Dilanian, and T. Sasaki, *Nature (London)* **422**, 53 (2003).
 - ² C. Martin, A. Maignan, D. Pelloquin, N. Nguyen, and B. Raveau, *Appl. Phys. Lett.* **71**, 1421 (1997).
 - ³ A. A. Taskin, A. N. Lavrov, and Y. Ando, *Phys. Rev. B* **71**, 134414 (2005).
 - ⁴ A. Maignan, V. Caignaert, B. Raveau, D. I. Khomskii, and G. A. Sawatzky, *Phys. Rev. Lett.* **93**, 026401 (2004).
 - ⁵ A. A. Taskin and Y. Ando, *Phys. Rev. Lett.* **95**, 176603 (2005).
 - ⁶ H. Wu, *J. Phys.: Condens. Matter* **15**, 503 (2003).
 - ⁷ Q. Zhang and W. Zhang, *Phys. Rev. B* **67**, 094436 (2003).
 - ⁸ H. Wu, *Phys. Rev. B* **64**, 092413 (2001).
 - ⁹ D. D. Khalyavin, *Phys. Rev. B* **72**, 134408 (2005).
 - ¹⁰ C. Frontera, J. L. García-Muñoz, A. Llobet, and M. A. G. Aranda, *Phys. Rev. B* **65**, 180405(R) (2002).
 - ¹¹ E. Sjöstedt, L. Nördstrom, and D. J. Singh, *Solid State Commun.* **114**, 15 (2000).
 - ¹² K. Schwarz and P. Blaha, *Comp. Mat. Sci.* **28**, 259 (2003).
 - ¹³ P. Blaha, K. Schwarz, G. K. H. Madsen, D. Kvasnicka, and J. Luitz, *WIEN2k, An Augmented Plane Wave Plus Local Orbitals Program for Calculating Crystal Properties. ISBN 3-9501031-1-2*, Vienna University of Technology, Austria (2001).
 - ¹⁴ J. P. Perdew, K. Burke, and M. Ernzerhof, *Phys. Rev. Lett.* **77**, 3865 (1996).
 - ¹⁵ A. I. Liechtenstein, V. I. Anisimov, and J. Zaanen, *Phys. Rev. B* **52**, R5467 (1995).
 - ¹⁶ A. G. Petukhov, I. I. Mazin, L. Chioncel, and A. I. Liechtenstein, *Phys. Rev. B* **67**, 153106 (2003).
 - ¹⁷ D. J. Singh, *Planewaves, pseudopotentials and LAPW method* (Kluwer Academic Publishers, 1994).
 - ¹⁸ M. A. Korotin, S. Y. Ezhov, I. V. Solovyev, V. I. Anisimov, D. I. Khomskii, and G. A. Sawatzky, *Phys. Rev. B* **54**, 5309 (1996).
 - ¹⁹ W. S. Kim, E. O. Chi, H. S. Choi, N. H. Hur, S. J. Oh, and H. C. Ri, *Solid State Commun.* **116**, 609 (2000).
 - ²⁰ C. Frontera, J. L. G.-M. noz, A. Llobet, M. A. G. Aranda, J. Rodríguez-Carvajal, M. Respaud, J. M. Broto, B. Raquet, H. Rakoto, and M. Goiran, *J. Alloy Compd.* **323-324**, 468 (2001).
 - ²¹ M. Respaud, C. Frontera, J. L. Garcia-Munoz, M. A. G. Aranda, B. Raquet, J. M. Broto, H. Rakoto, M. Goiran, A. Llobet, and J. Rodríguez-Carvajal, *Phys. Rev. B* **64**, 214401 (2001).
 - ²² A. Maignan, C. Martin, D. Pelloquin, N. Nguyen, and B. Raveau, *J. Solid State Chem.* **142**, 247 (1999).
 - ²³ E. Suard, F. Fauth, V. Caignaert, I. Mirebeau, and G. Baldinozzi, *Phys. Rev. B* **61**, R11871 (2000).
 - ²⁴ C. S. Knee, D. J. Price, M. R. Lees, and M. T. Weller, *Phys. Rev. B* **68**, 174407 (2003).
 - ²⁵ Z. Hu, H. Wu, M. W. Hackerfort, H. H. Heisch, H. J. Lin, T. Lorenz, J. Baier, A. Reichl, I. Bonn, C. Felser, et al., *Phys. Rev. Lett.* **92**, 207402 (2004).
 - ²⁶ H. Wu, *Phys. Rev. B* **62**, R11953 (2000).
 - ²⁷ J. Wang, W. Zhang, and D. Y. Xing, *Phys. Rev. B* **64**, 064418 (2001).
 - ²⁸ K. Knizek, P. Novák and Z. Jiráček, *Phys. Rev. B* **71**, 054420 (2005).
 - ²⁹ A. A. Taskin, A. N. Lavrov, and Y. Ando, *Phys. Rev. Lett.* **90**, 227201 (2003).
 - ³⁰ F. Fauth, E. Suard, V. Caignaert, and I. Mirebeau, *Phys. Rev. B* **66**, 184421 (2001).
 - ³¹ H. D. Zhou and J. B. Goodenough, *J. Solid State Chem.* **177**, 3339 (2004).
 - ³² W. R. Flavell et al., *Phys. Rev. B* **70**, 224427 (2004).
 - ³³ S. Roy, M. Khan, Y. Q. Guo, J. Craig, and N. Ali, *Phys. Rev. B* **65**, 064437 (2002).